Developing reliable and fast simulated annealing for stand-level forest harvesting schedule with virtual dimensionality reduction

Kai MORIGUCHI

Faculty of Agriculture and Marine Science, Kochi University

200 Otsu, Monobe, Nankoku, Kochi 783-8502 JAPAN

Tel: +81-88-864-5146

E-mail: k_moriguchi@kochi-u.ac.jp

Abstract

Identifying optimal harvesting (thinning and clearcutting) schedule for a forest stand (stand-level) is of great importance to forest managers and researchers. However, providing highly reliable optimal harvesting schedules still requires considerable computation time. This study aimed to develop a simulated-annealing-based method to provide a highly reliable optimal schedule for harvesting in a short time. In practice, the optimal number of harvesting events in a rotation may not be large. Therefore, 1) treating harvesting ages as well as the thinning intensity as control variables, and 2) searching the optimal number of thinning events iteratively, the dimension of the scheduling problem was virtually reduced. The method was developed through a comparison with a reliable method for a model with fixed harvesting ages. Three candidate neighborhood methods were developed and compared with each other. One neighborhood method was less robust than the other two methods. We further developed a method to optimize the planting density simultaneously with the harvesting schedule. Introduction of planting density as a control variable reduced computation time by decreasing the optimal number of harvesting for several cases. The developed method provided optimal schedules with much less time than the previous method for most cases.

Keywords

stand-level forest harvesting schedule; simulated annealing; neighborhood search; dimensionality reduction; soil expectation value

1 Introduction

Optimal forest harvesting (thinning and clearcutting) schedules for a given forest stand (stand-level) have been explored from various perspectives, such as increasing profitability of forestry (Ota et al., 2013), biodiversity conservation (Nghiem, 2014), and promoting carbon sequestration (Dong et al., 2020a). However, identifying an optimal forest harvesting schedule is complex, even with simple criteria such as the profitability of forestry. While longer rotation ages provide forest owners with a higher volume of yield at clearcutting, they can also decrease annual profit by slowing the land-use cycle and incurring loss of interest. Intraspecific competition caused by tree density results in smaller tree sizes but larger yields in dense stands. The forest owners often obtain yield harvested during commercial thinnings, which provides an income during early years and reduces the effect of interest loss. In contrast, the harvesting cost during thinning is higher than that during clearcutting. Thus, the stand-level harvest scheduling problem involves complex trade-off relationships.

Forest owners and managers are hard to intuitively design optimal harvesting schedules in their stands because of the complexity. Therefore, researchers have developed the computational methods to identify optimal schedules based on random search (Bullard et al., 1985), nonlinear programming (Roise, 1986), dynamic programming (Yoshimoto, 2003; Yoshimoto et al., 1990), and evolutionary methods (Xue et al., 2019) by comparing with each other. However, the objective function of the stand-level harvesting schedule is nonconvex and multimodal (Moriguchi et al., 2017). In other words, an "optimal" schedule can be a local optimum. A reliable method may be developed involving comparison with assured methods that produce solutions close to global optima.

A reliable method for the stand-level harvesting schedule optimization may only be developed by starting a comparison with a grid search. Moriguchi (2013) developed a grid search that computes all possible combinations of discretized thinning rates of given thinning ages. The comparison between the grid search, a random search, and a popular dynamic programming method for stand-level harvesting schedule named MSPATH (Yoshimoto et al.,

1990) showed that neither the random search nor the dynamic programming method could provide sufficiently optimal solutions. Although the grid search was the most reliable method, considerable calculation cost in the cases of long rotations and finer thinning rates limits practical availability. Therefore, Moriguchi et al. (2015, 2017) developed a reliable alternative method based on simulated annealing (SA) (Černý, 1985; Kirkpatrick et al., 1983) through comparison with the grid search. The latest method provides solutions that exceed those of the grid search with far fewer iterations (Moriguchi, 2020).

Even with these improvements, the method should be further enhanced for fast computation. Moriguchi (2020) reported that the latest method minimally requires over 30 seconds to provide solutions for a model which employs logging simulation, even using GPUs. If one needs the optimal harvesting schedule for a single stand, this time may be permissible. However, optimal stand-level harvesting schedules of many stands are often necessary to estimate supply potential or plan the use of forest resources in regions (Battuvshin et al., 2020; Matsuoka et al., 2021; Moriguchi, 2021). For such cases, the calculation time to provide optimal harvesting schedules is still unsuitably long.

It is noted that Moriguchi (2020) assumed an inefficient structure of the yield models so that the solutions were comparable to those of the grid search. The yield models fixes thinning ages to five-year increments, from minimum candidate thinning age to the rotation age (fixed age (FA) model: left plot of Fig. 1). However, actual forest owners limit the number of thinning events to reduce preparation costs, such as the cost for installing machines. Consequently, they rarely conduct commercial thinning every five years. Furthermore, harvesting ages are fundamentally continuous control variables (Arias-Rodil et al., 2015, 2017; Pasalodos-Tato & Pukkala, 2007) (variable age (VA) model: right plot of Fig. 1). Introducing these ages as well as thinning intensity as control variables can formally increase the number of control variables, i.e., model dimension. However, considering the limited number of thinning events in practice, the dimension may rather be reduced.

Additionally, optimal planting density is another concern in practice. Ota et al. (2013)

proposed the harvesting schedules for several plant densities and concluded that lower planting density could increase the soil expectation value (SEV). It is noted that planting density can be optimized simultaneously with the harvesting ages and thinning intensity (expanded variable age (EVA) model: dotted arrows in the right plot of Fig. 1). A reliable and fast method that addresses these issues will enhance the quality of studies and practical applications that utilize optimal forest management schedules.

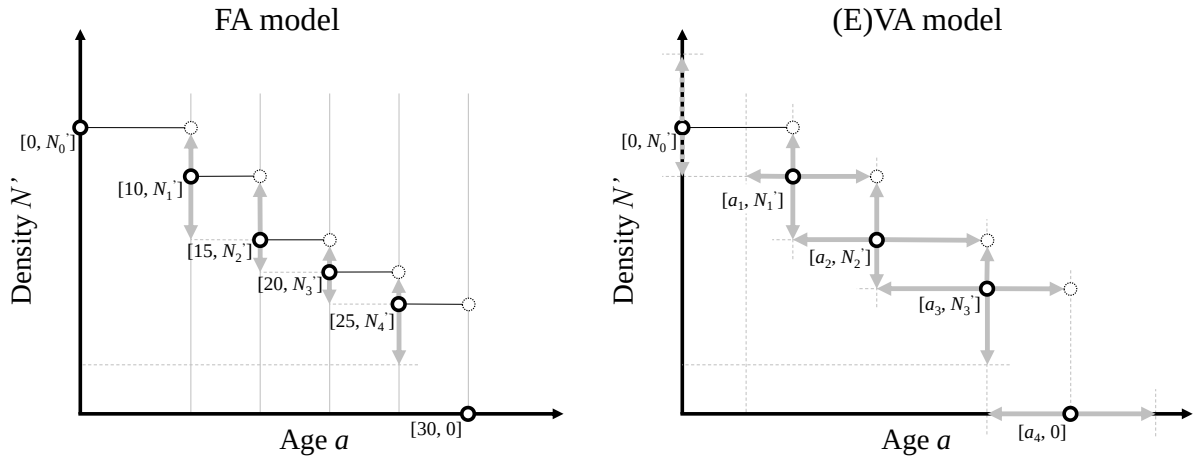

Fig. 1. The model structure of the optimization of stand-level forest harvesting schedule. [a_i, N'_i] denotes a set of the harvesting age (a) and virtual planting density[1] (N') after the ith harvesting age, respectively. The existing method fixes the candidate thinning ages and optimizes the set of N' values (left plot; fixed age (FA) model). The optimal rotation age is identified by changing the number of thinning events. The present method introduces the harvesting ages as control variables (right plot; variable age (VA) model). The expanded VA model (EVA) introduces planting density (N'_0) as a control variable (dotted arrows in the right plot).

This study developed an SA-based method to optimize a stand-level forest harvesting schedule and planting density addressing the two issues above. There were two matters to establish the method: I) identification of an effective neighborhood search method; and II)

[1] Assumed planting density to simulate the stand density at a given age (Moriguchi et al., 2015).

development of reliable method introducing optimization of planting density. There are multiple candidate neighborhood search methods when both harvesting ages and thinning intensity are control variables. Neighborhood search methods of SA often change the optimization performance (Bettinger et al., 2007; Dong et al., 2015). Therefore, we should identify the effective method. Furthermore, the model flexibility of the EVA model is quite different from the FA model. Therefore, we developed the method for the VA model by comparison with Moriguchi's (2020) method of the FA model first, then developed the method for the EVA model by comparison with that for the VA model.

2 Material and Method

2.1 Objective models

We used the benchmark yield models defined by Moriguchi (2020) for cedar (*Cryptomeria japonica*), cypress (*Chamaecyparis obtusa*), red pine (*Pinus densiflora*), and larch (*Larix kaempferi*) of the Nagano Prefecture, Japan, with a few modifications. The objective was to maximize the soil expectation value (SEV; yen/ha), the net present value under an infinite repeat of rotations with a given harvesting schedule:

$$\text{Maximize SEV} = \sum_{r=0}^{\infty}\left[\left(\sum_{i=1}^{n} P_i\delta^{-a_i}\right) - C\right]\delta^{-Ar} = \frac{\sum_{i=1}^{n} P_i\delta^{-a_i} - C}{1-\delta^{-A}}, \quad (1)$$

where n is the number of harvests in a rotation, i denotes the index of harvesting, P_i is the profit at ith harvesting (yen/ha), δ is the annual discount given as $1/(1+0.01I)$ with I % annual interest rate, a_i is the age for conducting the ith harvest (year), C is the net present value of planting and silviculture costs (yen/ha), and A is the rotation age (year), which is the year of clearcutting and therefore $A = a_n$.

Moriguchi's (2020) model fixes the ages for harvesting at five-year intervals, and the virtual planting densities after ith harvesting (N'_i) is optimized to maximize the SEV (the FA model). The FA model and the optimization method for the model in this study were the same as those of Moriguchi (2020). The FA model directly associates the rotation age with n. Therefore, the

optimal rotation age was explored by identifying the optimal solution for each n first, then selecting the best solutions from them. Practical rotation age can be less than 10 years but often greater than 100 years (Katakura et al., 2005; Koskela et al., 2007; Nghiem, 2014). Consequently, the maximum n should not be a small number. The range of n in this study was from 1 to 21 (rotation age: 10 to 110 years). There were two types of yield models. One calculates the harvest simply by valuing the standing trees according to the diameter of trees at 1.2 m height (simple yield: SY). Another simulates the logging process (logging yield: LY). Further, there were two variations of clearcutting cost: full cost (F) and half cost (H). As a result, four yield models were defined for each species. For more detail, see Moriguchi (2020). SY and LY models were distinguished in our analysis because the logging simulation adds substantial complexity to the model. In contrast, the difference between F and H variations was treated similarly to that between species.

The solutions of the FA model were comparable to those of the grid search because of the fixed harvesting ages. However, the model structure is fundamentally inefficient. The VA model allows the harvesting ages to be control variables, thereby resolve the inefficiency. We need to explore the optimal values of a_i and N'_i for the VA model (right plot of Fig. 1). Therefore, the VA model has double the number of variables of the FA model for a given n value. Furthermore, we need to find optimal solutions by changing n to identify the optimal number of thinning events even for the VA model. However, because the rotation age is also a variable, long rotation age can be treated by using only a few control variables. For example, $a_1 = 100$ for $n = 1$ indicates the harvesting schedule without thinning that sets the rotation age to 100. Instead, the number of commercial thinning events is limited in practice. As a result, we can set the maximum n to a smaller value than in the FA model. The range of n of the VA model was from 1 to 10 in this study. The VA model replaces the constraint of $a_i = a_1 + 5(i - 1)\ \forall i$ of the FA model (Eq. (S5) in Supplementary Data 1 of Moriguchi (2020)) with Eq. (3) in Section 2.2. The EVA model further replaces the constraint of $N'_0 = x$ (x = 3,000 trees/ha for cedar and cypress; x = 2,500 trees/ha for larch and pine) with the constraint of Eq. (4) in Section 2.2.

Moriguchi (2020) used a fixed regeneration cost, assuming a fixed planting density for each species. We modified the regeneration cost into the form of $c + u \cdot N'_0$, where c is the fixed cost of regeneration (yen/ha), and u is the unit cost of planting a sapling (yen/tree), according to the standard cost table of regeneration (Nagano Prefectural Government, 2020). The values were set to c = 928,070 yen/ha, u = 128.3 yen/tree for cedar, c = 931,570 yen/ha, u = 128.3 yen/tree for cypress, c = 806,725 yen/ha, u = 108.7 yen/tree for larch, and c = 687,437 yen/ha, u = 102.8 yen/tree for pine.

2.2 Neighborhood search methods

Neighborhood search methods cause optimization performance (Bettinger et al., 2007; Dong et al., 2015). For the FA model, generating a candidate N'_i values using the bounds of Eq. (2), rather than using the thinning rate at each age as variables, is an effective control (Moriguchi et al., 2017):

$$\begin{aligned} &\max\{N'_{i+1}, N'_{i-1}(1-R_{\max})\} \le N'_i \le \min\{N'_{i-1}, N'_{i+1}/(1-R_{\max})\}, \quad \forall i \in \{1,2,\dots,n-2\}, \\ &\max\{N'_{\min}, N'_{n-2}(1-R_{\max})\} \le N'_{n-1} \le N'_{n-2}, \qquad\qquad ,i = n-1, \end{aligned} \tag{2}$$

where $R_{\max}$ is the maximum thinning rate (0–1), and $N'_{\min}$ is the minimum N'_i. Note that N'_n is always zero because of clearcutting. $N'_i = N'_{i+1}$ simulates a skip of commercial thinning at a given age. If the initial N'_i values satisfy the constraints of Eq. (2), generated solutions in the SA process are always feasible. Therefore, we can avoid the use of a barrier function for N'_i values. We used the same neighborhood method of Moriguchi (2020) to search for optimal N'_i values of the VA and EVA models as well as the FA models.

The VA and EVA methods allow the harvesting ages, a_i, to be control variables. An effective method of generating candidate ages may ideally be explored as done for N'_i. However, the optimizations of N'_i and a_i have a similar structure in the VA and EVA models: the optimization of the point positions (right plot of Fig. 1). Therefore, in this study, we used the following bounds to generate candidate harvesting ages:

$$\begin{aligned} a_{\min} \le a_1 \le a_2 - \Delta a, \\ a_{i-1} + \Delta a \le a_i \le a_{i+1} - \Delta a \quad \forall i \in \{2,3,\dots,n-1\}, \\ a_{n-1} + \Delta a \le a_n \le a_{\max}, \end{aligned} \tag{3}$$

where $a_{\min}$ and $a_{\max}$ are the lower and upper bounds of harvesting ages (year), respectively, and Δa is the minimum interval between thinning. In this study, $a_{\min}$ = 10, $a_{\max}$ = 110, and Δa = 5. If the initial a_i values satisfy the condition of Eq. (3), the constraints keep the order of a_i, i.e., $a_1 < a_2 < \dots < a_n$, and the interval equal to or more than Δa (year). Therefore, we can avoid the use of a barrier function for a_i values as well as for N'_i values.

The planting density (N'_0, tree/ha) of the EVA model was generated in the following range:

$$\max\{N'_1, N'_{\min}\} \le N'_0 \le N'_{\max}, \tag{4}$$

where $N'_{\min}$ and $N'_{\max}$ are the lower and upper bounds of N'_i values (trees/ha), respectively. In this study, $N'_{\min}$ = 1,000 yen/ha, and $N'_{\max}$ = 10,000 yen/ha. If the initial N'_0 value is in the range, generated solutions in the SA process are always feasible.

We focused on the order of updates of N'_i and a_i. There are multiple possible orders for updating the variables. We defined three types in this study (Fig. 2):

Type A: Update each a_i one by one, then update each N'_i one by one, such that $a_1 \to a_2 \to \dots \to a_n \to N'_1 \to N'_2 \to \dots \to N'_{n-1} \to \dots$ (for the VA model)

Type B: Update a_i and N'_i alternately, such that $a_1 \to N'_1 \to a_2 \to N'_2 \to \dots$

Type C: Update the sets of a_i and N'_i, such that $[a_1, N'_1] \to [a_2, N'_2] \to \dots \to [a_n, 0] \to \dots$

For the EVA model, type A updates N'_0 before the update of N'_1, and type B updates N'_0 before a_1. Type C updates N'_0 before the update of $[a_1, N'_1]$ as $[0, N'_0]$. Thus, type C does not update N'_0 with a_n. Thus, Types A and B change one variable per iteration in an SA process, and type C changes two variables at once.

Moriguchi et al. (2017) recommended the use of truncated Cauchy distribution to generate candidate values, no scale of the distribution depending on the temperature parameter of SA, and exponential cooling schedule of the temperature parameter for the FA model. Moriguchi (2020) introduced additional scaling processes for N'_i to help generate solutions of few thinning. SA is sensitive to the setting of meta-parameters, such as cooling rate or the starting and final

temperature (Dong et al., 2020b). To deal with this feature, Moriguchi (2020) introduced a meta-optimization of the SA parameters using a hybrid method of tabu search and direct search. We used the method of Moriguchi (2020) in these aspects.

In conclusion, the solutions of the FA model were produced using Moriguchi's (2020) method. The solutions of the VA model were produced by introducing harvesting ages as control variables that were generated in the bounds of Eq. (3). The EVA model further introduced planting density as a control variable, and the candidate value was generated in the bounds of Eq. (4). The VA and EVA models have neighborhood search types A-C. The three types were compared in this study.

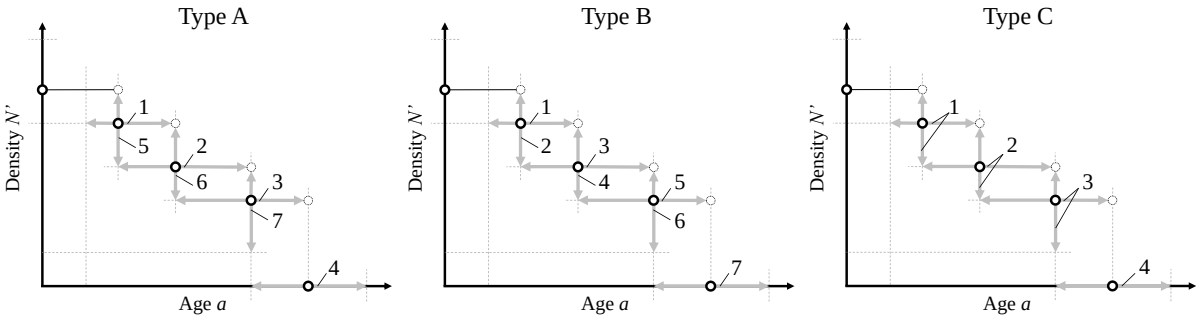

Fig. 2. Three types for updating the variables. An example case of n = 4 of the VA model. The values on the arrows indicate the order of updates. Type A updates each a_i one by one, then updates each N'_i one by one. Type B updates a_i and N'_i alternately. Type C updates the sets of a_i and N'_i.

2.3 Investigation process

Moriguchi (2020) reported that the method for the FA model could provide solutions with higher SEVs than those of the grid search with much fewer iterations for all the tested cases. Therefore, we developed the objective method for the EVA model through comparison with Moriguchi's (2020) method. However, direct comparison between the solutions of the EVA and FA models is difficult because of substantial differences in model structures: the FA model fixes both thinning ages and planting density while the EVA model allows both to be variable. The flexibilities of the FA model and the VA model are also different. The FA model can provide higher SEVs than the VA

model because of larger n. In contrast, the VA model is also possible to provide solutions with higher SEVs because of variable harvesting ages. Even with this situation, we may be confident that the present methods for the VA model offer reliable solutions if the methods provide solutions with higher SEVs than the FA model for a given yield model. Similarly, the methods for the EVA model were developed through comparison with the grid search on planting density using the methods for the VA model. If the methods for the VA model are reliable, the grid search on planting density may provide satisfactory solutions to confirm the reliability of methods for the EVA model. Because the EVA model has higher flexibility than the VA model, we expected the methods for the EVA model to provide better solutions than the grid search on planting density.

We first compared the solutions of the VA model with those of the FA model. The highest SEVs at each n for each yield model using types A-C was identified. For each n, the method ran at least 5000 SA processes at 10^7 iterations per SA process (using at least 125 SA parameter sets, each with 40 processes, resulting in 5×10^{10} ($=10^7 \times 125 \times 40$) calculations of SEV). Note that the meta-optimization of the SA parameters may further increase the calculations. The highest SEV for each n of a given yield model was defined as hSEV. The hSEV was used to analyze the optimization performance and necessary iterations for each n of types A-C of the VA model. We also defined HSEV as the maximum SEV found for a given yield model. The HSEV of a given yield model is the highest hSEV of all n values. The values of HSEVs vary with the yield models. Therefore, we analyzed the results using the difference of SEV from the HSEV of each yield model.

For optimization models with fixed dimensions, statistical tests using extreme value distributions are often used to estimate whether the solutions are sufficiently close to the global optima (Bettinger et al., 2009; Dong et al., 2015; Moriguchi et al., 2020). In contrast, applying the method to the stand-level harvesting schedule causes complications because the optimization of n, the model dimension itself, is involved. The dynamic meta-optimization of the SA parameter also complicates the set of solutions for the statistical tests. Therefore, we compared the highest SEVs of types A-C with each other instead. By analyzing the variations of the SEVs, we evaluated

whether the solutions with HSEVs were close to the global optima.

We then constructed the models of the necessary number of iterations to offer acceptable solutions. The acceptable solutions were defined by setting the tolerance (decrease) of the resultant SEV of each n from hSEV to 1,000 yen/ha, which is less than one hour wage for a logging worker. The candidate number of iterations per SA process is 10^x, with x from 2.25 to 7 in increments of 0.25, yielding 20 candidates. The necessary number of iterations for each n is defined similarly to a previous study (Moriguchi, 2020): the number of iterations that provides acceptable solutions for all the yield models, while the relationship between the number of iterations and n is convex.

We developed the methods for the EVA model with a similar approach. The grid search on planting density using the methods for the VA model was used to ensure the reliability of the methods for the EVA model. The grid search discretized the planting density from 1,000 trees/ha to 10,000 trees/ha by 100 trees/ha. We first identified the hSEV and HSEV of each yield model and compared the highest SEV of types A-C. We then identified the necessary number of iterations for each n, allowing 1000 yen/ha decrease from the hSEV.

Finally, we evaluated the calculation cost to provide satisfactory solutions for the VA and EVA models. The cumulative numbers of iterations for providing an optimal harvesting schedule at searching for optimal n in ascending order were analyzed. The calculation time to provide the solution on a computer was also reported. The time measurement was replicated ten times. All the investigations were conducted using the code set written in CUDA 11.1 and C++17. The program was compiled with Visual Studio 2019 (Microsoft) with O2 optimization for both CUDA and C++17 with the fast-math option. The program was run on a computer with a TITAN-V GPU (nVIDIA) and a Xeon E5-2697-v3 CPU (Intel).

3 Results and Discussion

3.1 Methods for the VA model

3.1.1 Solutions of the VA model

The harvesting schedules that provided the HSEVs for the VA model are presented in Supplementary Table S1. The differences between the HSEVs and the highest SEVs obtained using each method are presented in Fig. 3. Note that the vertical axis is a logarithmic scale. Expect for Pine-F of the LY model, types A-C for the VA model always provided much higher SEVs than the method for the FA model. The highest SEVs identified using the FA model differed from the HSEVs by up to 40,126 yen/ha (Cypress-H of the SY model). In contrast, the variation of the highest SEVs found using types A-C was up to 10.5 yen/ha (for Pine-H of the LY model; type C provided 10.5 yen/ha lower SEV than type A). For Pine-F of the LY model, the FA model provided the solution with HSEV, and types A-C for the VA model provided solutions with 119.4-120.9 yen/ha less SEVs. The HSEV was identified with n = 10 for eight cases (Supplementary Table S1). In contrast, hSEVs with a decrease from HSEV within 200 yen/ha was found with $n \leq 6$ for all models.

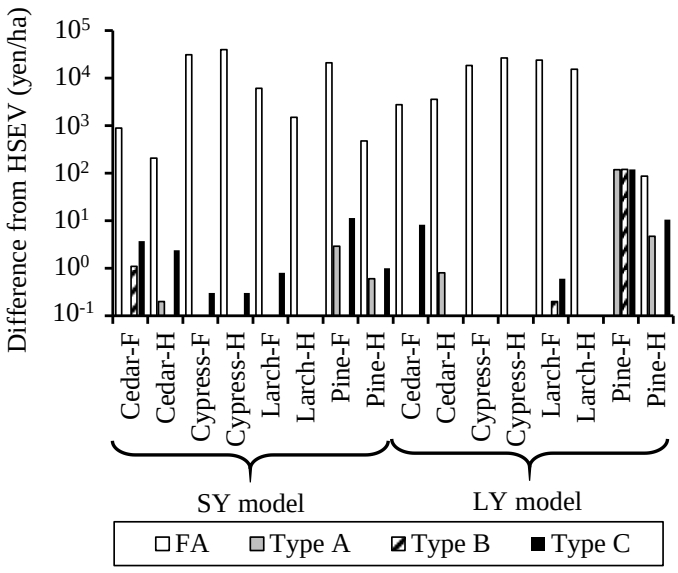

Fig. 3. Differences between the HSEVs and the highest SEVs provided by the method for the FA

model and types A-C for the VA model. Note that the vertical axis is a logarithmic scale.

The lower SEVs of the FA model for almost all cases are natural because the FA model has less flexibility in the choice of harvesting ages than the VA model. On the other hand, the FA model allows harvestings every five years and up to a maximum of 21 times. Thus, if intense thinning with short intervals is advantageous, the FA model can provide higher SEVs than the VA model. The result of Pine-F of the LY model provided such a scenario: the FA model suggested harvesting at every thinning candidate age with low thinning rates until the maximum rotation age. However, such intensive thinning for over a century may not be practical because preparation for thinning is costly. The yield models use simple harvesting cost value per harvested volume and do not distinguish between the preparation costs and the cost of harvesting. This feature of the yield model allows the FA model to provide a higher SEV than the VA model. Note that, even for Pine-F of the LY model, types A-C of the VA models offered solutions that were close to the HSEV with a limited number of thinnings. Therefore, the results of Pine-H of the LY model do not indicate problems of types A-C for the VA model. Instead, the low variation between the highest SEVs of types A-C suggests that those types can provide reliable optimal solutions for the VA model if we use 10^7 iterations per SA process. Consequently, the resultant HSEVs may be close to the SEVs of the global optima.

Fig. 4 presents the change of hSEVs with n of the VA model. In all the yield models, once the hSEVs approach the HSEVs with $n \leq 6$, the hSEVs do not change for several n. For the larch yield models, the hSEVs decrease when $n > 6$. In contrast to the FA model, n of the VA model does not indicate the rotation age directly. However, n is indirectly associated with rotation age due to the constraint of the minimum thinning interval. Therefore, an overly large n can prevent the selection of an optimal rotation age. Consequently, the decreases in the hSEV with large n values are natural for cases in which optimal rotation ages are relatively short (50.9 years and 39.3 years for Larch-F and Larch-H of the SY model; 56.5 years and 44.5 years for Larch-F and Larch-H of the LY model). A cause of the constant hSEV even with different n was the case of N'_i =

322 N'_{i+1} (0% thinning). Fig. 5 presents the optimal harvesting schedule of Larch-H of the SY model
323 with n = 3 and n = 6. The harvesting schedule of n = 6 reproduced that of n = 3 by setting the
324 thinning rate to 0% at the grey arrows. As a result, the hSEVs rarely changed with n for similar
325 cases. In fact, some optimal solutions in Supplementary Table S1 also show a series of similar
326 values.

327 These results indicate a practical use of the method: the optimal n can be explored
328 sequentially from the small number. If the maximal SEV does not change or decrease with n, the
329 search for an optimal harvesting schedule for a larger n can be avoided. The ordinary method for
330 the FA model also suggested such a reduction in the search for an optimal n (Moriguchi, 2020).
331 However, n of the FA model is directly associated with rotation age due to fixed thinning ages.
332 Therefore, if the optimal rotation age can be a large value, the optimization for large n values
333 cannot be omitted. In contrast, the VA model can treat a long rotation age with a small n due to
334 variable harvesting ages. Considering that the number of thinning events per rotation is limited
335 in reality, the use of the VA model, thereby enabling reduced searching for large n values, may be
336 more efficient than the use of the FA model.

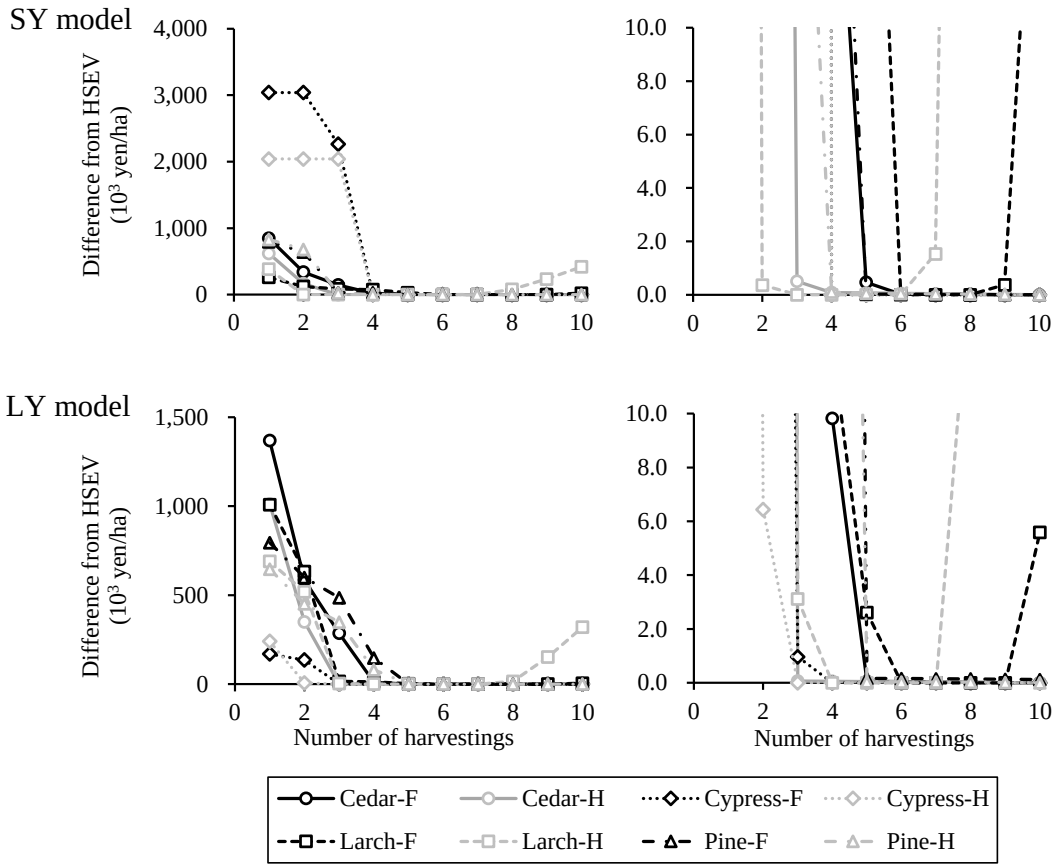

Fig. 4. The change of hSEVs with *n* for the VA model. The vertical axes of the left plots cover the range of the values. Right plots are enlarged versions of the left plots with the vertical axes scaled. Note that the large difference from HSEV indicates lower SEV.

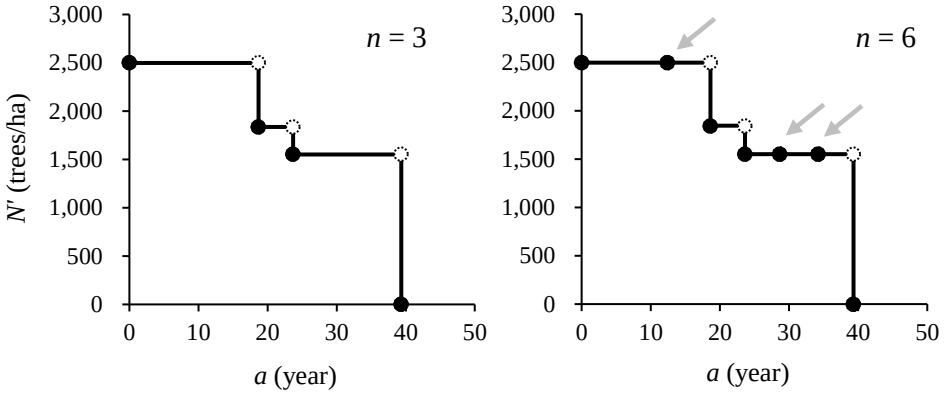

Fig. 5. The optimal harvesting schedules for *n* = 3 and *n* = 6 for Larch-H of the SY model. The harvesting schedule of *n* = 6 used approximately 0% thinnings at the grey arrows.

3.1.2 Iteration models of the VA model

The necessary numbers of iterations to find acceptable solutions (the decreases of SEVs from hSEVs are less than 1,000 yen/ha) for each n are presented in Fig. 6. Type C failed to find a solution that satisfies the tolerance for the case of n = 9 for Larch-H of the LY model even with 10^7 iterations. Note that the necessary number of iterations for type C for the LY models ignores the failure and therefore provides an underestimate. In other cases, acceptable solutions were found with up to $10^{6.75}$ iterations. Comparing the total number of iterations to offer the optimal harvesting schedule for a yield model by full calculation from n = 1 to n = 10, type A was the fastest method of the SY models (type A: 905,182; type B: 1,176,872; type C: 1,938,246). For the LY models, type B required fewer iterations than type A (type A: 15,290,098; type B: 10,084,319). The number of iterations of type C for the LY models was 5,032,106 if it did not fail to find an acceptable solution.

This result indicates that types A and B may be relatively robust compared with type C. However, we noted that the rotation age of Larch-H of the LY model was 44.5 years. The selection of the rotation age was prevented when n = 9. Furthermore, type C could provide sufficient solutions with a relatively small number of iterations for other cases of the LY models. Therefore, we did not reject type C at this point and used all the three types for the grid search on planting density.

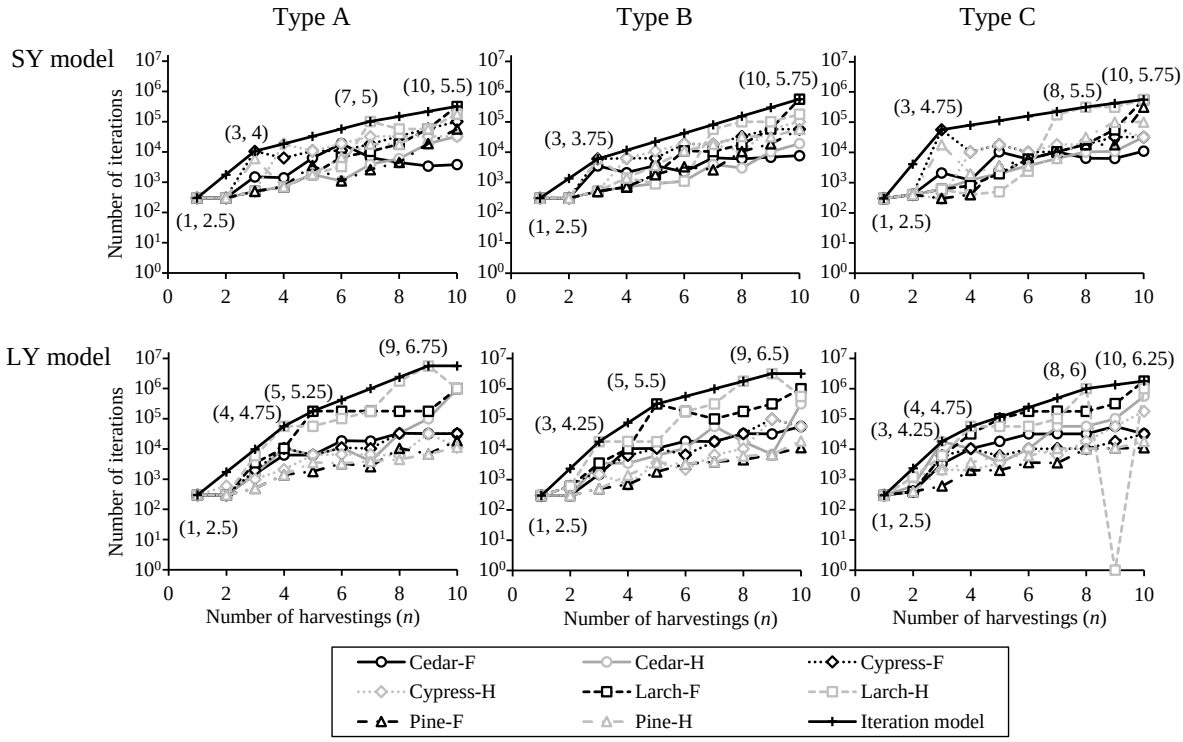

Fig. 6. The number of iterations to find solutions within 1,000 yen/ha decrease of SEV from hSEV for the VA model. The coordinate values in parentheses are the edges of the models for the necessary number of iterations. The plot at 10^0 indicates a failure to obtain a solution that satisfies the tolerance.

3.2 Method for the EVA model

3.2.1 Solutions of the EVA model

The harvesting schedules that provided the HSEVs for the EVA model are presented in Supplementary Table S1. The differences between the HSEV and the highest SEV of each method obtained using 10^7 iterations per SA process are presented in Fig. 7. The values of the "VA grid" indicate the highest SEV of the grid search on planting density using types A-C for the VA model. The value of the "VA grid" of each yield model was calculated as follows:

$$\max_{t,N_0'} SEV^*_{t,N_0'} \ , \tag{5}$$

where t is the neighborhood search method in {A, B, C} and N'_0 is the discrete planting density (trees/ha) in {1000, 1100, ..., 10,000}.

For each case, one of the types A-C for the EVA model provided the HSEV. The differences between types A-C in the highest SEVs were up to 7.4 yen/ha (between types A and C in Pine-H of the LY model). hSEVs with a decrease from HSEV within 200 yen/ha was found with $n \leq 5$ for all the yield models. In contrast, the grid search using the VA model had up to 10,966 yen/ha decrease in SEV from the HSEV. For Cedar-F of the LY model, the grid search on planting density with the VA model also provided the HSEV because the optimal planting density was just 1,000 trees/ha.

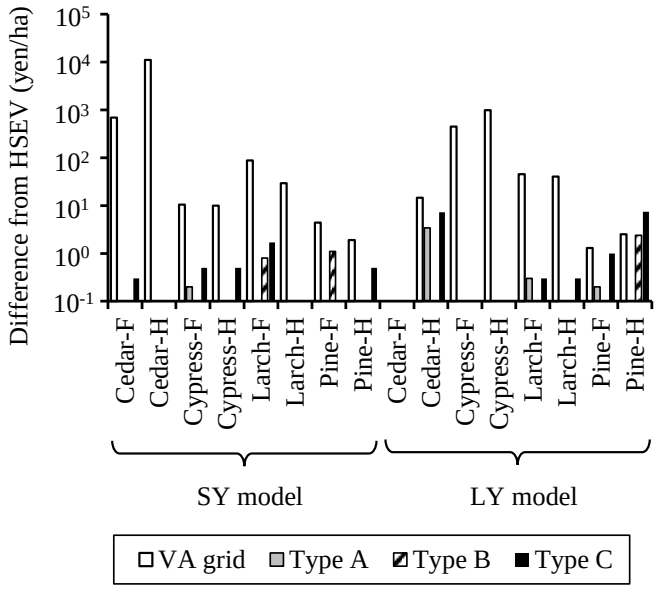

Fig. 7. Difference between the HSEVs and the highest SEVs provided by the methods for the EVA model. Note that the vertical axis is a logarithmic scale. The values of "VA grid" indicate the highest SEVs of grid search on planting density using types A-C of the VA model.

3.2.2 Iteration models of the EVA model

The necessary numbers of iterations to provide acceptable solutions are shown in Fig. 8. Type C again failed to provide an acceptable solution for Larch-H of the LY model when n = 9. The necessary number of iterations of a given n was generally larger than that for the VA model in Fig. 6. The models of the necessary number of iterations were similar among types A-C. Rather, the

difference between the SY and LY models was clear. LY models need larger numbers of iterations than SY models due to the complexity of the yield model. Types B and C required 10^7 iterations for LY models when $n \geq 8$, while type A required $10^{6.75}$ (5,623,413). The total number of iterations to offer the optimal harvesting schedule of the SY model by a complete run from $n = 1$ to $n = 10$ of types A-C were 2,803,887, 2,243,543, and 2,011,223, respectively. Thus, type C was the fastest method for the SY model. For the LY models, the total numbers of iterations of types A and B were 19,859,438 and 34,699,289, respectively.

Larch-H of the LY model with $n = 9$ again caused the failure of type C. The optimal rotation age of the yield model was 44.5 years ($n = 3$). Therefore, the prevention of selecting the optimal rotation age is a potential cause of the failure. However, we can at least conclude that types A and B are more robust than type C because the types could provide acceptable solutions for all the cases.

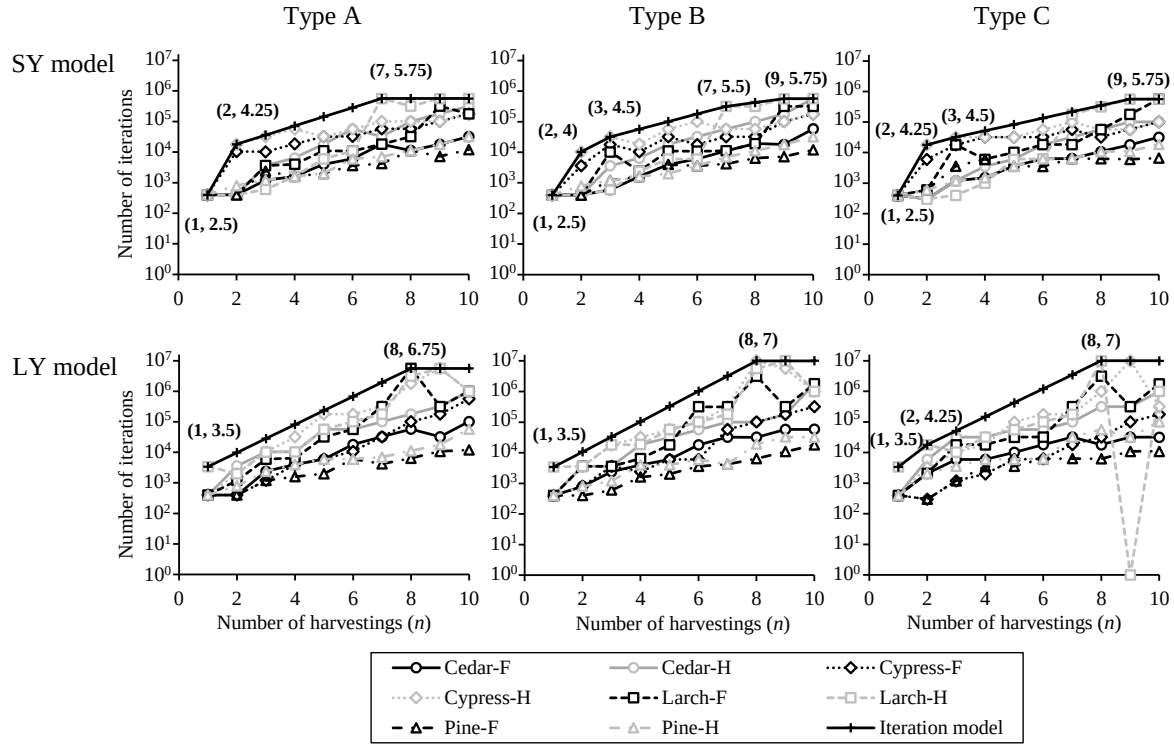

Fig. 8. The number of iterations to find solutions within 1,000 yen/ha decrease of SEV from hSEV for the EVA model. The coordinate values in parentheses are the edges of the models for the necessary number of iterations. The plot at 10^0 indicates a failure to obtain a solution that satisfies

413 the tolerance.

414

415 ### 3.3 Calculation cost

416 Fig. 9 presents the cumulative number of iterations of types A and B that were calculated using
417 the necessary numbers of iterations in Fig. 6 and Fig. 8, assuming that the optimal *n* is explored
418 sequentially in ascending order. Note that type C was omitted because of less robust
419 performance. The number of iterations is presented as the ratio between the value of
420 Moriguchi's (2020) method applied from $n = 1$ to $n = 21$. This comparison base was chosen
421 because the FA model may need to evaluate all the candidate *n* values in most practical cases to
422 find optimal rotation age. For all cases, the curves of types A and B were similar to each other.
423 Both types required fewer iterations when *n* was set to less than nine at using the VA model.
424 Even for the EVA model, both types reduced the number of iterations when *n* was less than seven.
425 In contrast, if *n* is a larger value, types A and B can require longer calculation time.

426 Because the hSEVs whose differences from HSEVs were less than 200 yen/ha were
427 identified when $n \leq 6$ for the VA models and $n \leq 5$ for the EVA models, both types may reduce the
428 calculation cost compared to Moriguchi's (2020) method in practical cases. The similarity
429 between the curves of types A and B suggests that those performances were similar. For $n = 10$,
430 type A required fewer iterations for the SY model of the VA model and the LY model of the EVA
431 model. Type B was the faster method for the other models. However, exploring optimal solutions
432 up to $n = 10$ may not be usual when introducing termination of the optimization process for
433 large *n* values with VA and EVA models. Therefore, a comparison in respect of calculation time
434 for real situations was in order.

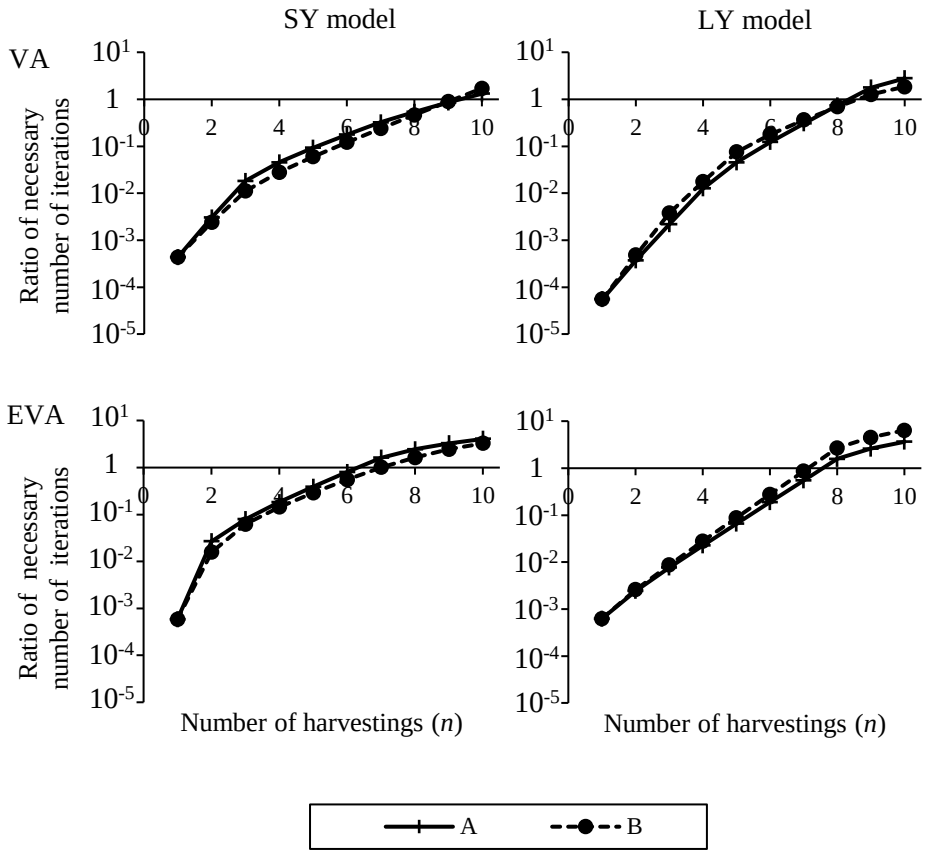

435

436 **Fig. 9. Cumulative number of iterations for types A and B.** The values are presented in a ratio
437 compared with the necessary number of iterations for the case of n = 21 of the FA model (Moriguchi,
438 2020).

439

440 Table 1 presents the mean calculation times required to provide acceptable solutions using
441 models of the numbers of iterations in Fig. 6 and Fig. 8. The optimization process increased n
442 sequentially, and if the increase of SEV with n was less than 1000 yen/ha twice, the optimization
443 process was terminated. While the mean calculation times vary with the yield model, both types
444 A and B provided the solutions on average within 0.76 s and 0.59 s, respectively, for the SY
445 models of the VA model. For the SY models of the EVA model, types A and B provided the
446 solutions within an average of 1.86 s and 1.28 s, respectively. Similarly, types A and B
447 respectively provided the solutions within an average of 12.85 s and 13.78 s for the LY models of
448 the VA model and within 3.62 s and 4.53 s for the LY models of the EVA model.

449

Moriguchi's (2020) method with the FA models required 2.251–5.330 s and 33.044–53.009 s for the SY and LY models using GPU, respectively. Compared with these values, the calculation times in Table 1 show much lower values in most cases. This difference is partly because Moriguchi's (2020) values included the complete calculation for all the candidate n values because the FA model was used. The optimal rotation changes with prices and cost (Williams & Nautiyal, 1990). Therefore, long rotation age is often considered and implemented in practice; for this case, the full calculation from n = 1 to n = 21 is required. In contrast, the number of thinning events is limited to avoid preparation costs in practice; therefore, we introduced a termination of the calculation for large n values. As a result, although Fig. 9 suggests that the developed method may require more time than Moriguchi's (2020) methods for large n values, the case is limited, and the actual calculation time is expected to be similar to the values in Table 1.

Because a large n requires more iterations, the reduction of n strongly affects the actual calculation time. In Table 1, the calculation times for the LY models using the EVA model was considerably less time than those of the VA model. It is noted that the optimization process for the EVA model was terminated with fewer n values. The harvesting schedules that provided the HSEV for the EVA model accepted low plant densities (Supplementary Table S1), and consequently, the optimal number of thinning was decreased. Thus, the introduction of planting density as a control variable can reduce the calculation time under similar circumstances.

Such a reduction in actual calculation time may be significant for practical use. Moriguchi (2020) introduced the GPGPU technique and enabled at least 12.7 times faster computation. The acceleration rate indicates the reduction of computation time is significant. However, at least 33 s was required to provide an optimal solution for the LY model even using a GPU. If stand-level optimal harvesting schedules for numerous stands are required, the calculation time was impractical. The present method may reduce practical calculation time while assuring reliability

477 and introducing optimization of planting density. Therefore, the present method is more readily
478 applied in practice.

479 Further reduction of computation time may be possible by introducing real constraints. The
480 present study used a range of thinning rates of 0%-50%. As a result, the search for an optimal *n*
481 is redundant in cases of virtually no thinning (illustrated in Fig. 5). The range of thinning rate
482 was necessary for comparison with the FA model. The FA model can simulate the absence of
483 thinning at a given age only by using 0% thinning rate because of fixed age. However, it was not
484 necessary for the VA and EVA models. Even if a solution indicates a very little thinning rate (e.g.
485 1%) at an age, it is not practical because most of the costs for harvesting should be paid with the
486 gain obtained by selling the logs. For example, Bettinger et al. (2005) introduced the minimum
487 harvest volume to avoid impractical low thinning intensity. Similarly, when we use the VA and
488 EVA models, setting the minimum thinning rate to non-zero is highly recommended for efficient
489 optimization and higher realism of the solutions. It is also noted that our investigation imposed
490 types A-C for the VA and EVA models to identify the optimal solution with sequential virtual
491 no-thinning for large *n* values (Fig. 5). The generation of a sequential no-thinning schedule is
492 rare when using the neighborhood search of Eq. (2) and decreases the optimization performance,
493 though additional scaling processes for N'_i relax the problem (Moriguchi, 2020). However,
494 imposing the identification of solutions with such a sequential virtual no-thinning is unnecessary
495 for the VA and EVA models. Therefore, the number of iterations presented in this study might be
496 overestimated than actual cases.

497 The virtual no-thinning may also be avoided by introducing the preparation cost of thinning
498 into the yield model. The yield model in this study used fixed thinning costs per volume and did
499 not consider the preparation costs. By introducing a preparation cost, the increment of *n* can
500 involve the additional preparation cost. It complicates the method to treat the skip of thinning
501 with the FA model. However, the VA and EVA models have no similar barrier. Rather, the hSEV
502 will change with *n* more radically than in our example (Fig. 4) and help identify the optimal *n*
503 value. Thus, introducing non-zero minimum thinning rates and preparation costs may allow

faster identification of the optimal harvesting schedules as well as improve the reality of the yield model.

4 Conclusion

We developed a method to provide reliable optimal solutions for stand-level forest harvesting schedules. Compared with Moriguchi's (2020) method for the FA model, the developed neighborhood search methods for the VA model successfully provided solutions with higher SEVs except for Pine-F of the LY model. This exception was due to the impractical intense thinning schedule indicated by the FA model. The method for the EVA model provided solutions with higher SEVs than the grid search on planting density using the methods for the VA model. Because Moriguchi's (2020) method for the FA model has an empirical assurance to provide better solutions than the grid search, we can be confident that the methods for the VA and EVA models will provide reliable optimal solutions. Practical calculation time was also reduced due to the virtual dimensionality reduction by using the VA and EVA models and introducing planting density as a control variable. Thus, the developed method provides higher performance than existing methods with respect to both reliability and calculation time. Our investigation allowed for a 0% minimum thinning rate and the yield model without preparation costs. However, these settings are not ideal for computation efficiency and less realism of the thinning operations. Introducing a non-zero minimum thinning rate and a preparation cost per thinning event may further reduce practical calculation time by helping efficient termination of optimization for larger n values as well as increasing the realism of the solutions. Assurance of reliability of more real yield models introducing non-zero minimum thinning rate and preparation costs may be a future work to be conducted.

Acknowledgments

This work was supported by the Japan Society for the Promotion of Science KAKENHI [grant

numbers 19K15872, 21H03672]. I am also grateful for insightful comments from two anonymous reviewers.

References

Arias-Rodil, M., Pukkala, T., González-González, J. M., Barrio-Anta, M., Diéguez-Aranda, U., 2015. Use of depth-first search and direct search methods to optimize even-aged stand management: a case study involving maritime pine in Asturias (northwest Spain). Can. J. For. Res. 45, 1269–1279. https://doi.org/10.1139/cjfr-2015-0044

Arias-Rodil, M., Diéguez-Aranda, U., Vázquez-Méndez, M. E., 2017. A differentiable optimization model for the management of single-species, even-aged stands. Can. J. For. Res. 47, 506–514. https://doi.org/10.1139/cjfr-2016-0237

Battuvshin, B., Matsuoka, Y., Shirasawa, H., Toyama, K., Hayashi, U., Aruga, K., 2020. Supply potential and annual availability of timber and forest biomass resources for energy considering inter-prefectural trade in Japan. Land Use Policy 97, 104780. https://doi.org/10.1016/j.landusepol.2020.104780

Bettinger, P., Graetz, D., & Sessions, J. (2005). A density-dependent stand-level optimization approach for deriving management prescriptions for interior northwest (USA) landscapes. For. Ecol. Manag. 217, 171–186. https://doi.org/10.1016/j.foreco.2005.05.060

Bettinger, P., Boston, K., Kim, Y.-H., Zhu, J., 2007. Landscape-level optimization using tabu search and stand density-related forest management prescriptions. Eur. J. Oper. Res. 176, 1265–1282. https://doi.org/10.1016/j.ejor.2005.09.025

Bettinger, P., Sessions, J., Boston, K., 2009. A review of the status and use of validation procedures for heuristics used in forest planning. Math. Comput. For. Nat. Sci. 1, 26–37. https://mcfns.net/index.php/Journal/article/view/MCFNS.1-26

Bullard, S. H., Sherali, H. D., Klemperer, W. D., 1985. Estimating optimal thinning and rotation for mixed-species timber stands using a random search algorithm. For. Sci. 31, 303–315. https://academic.oup.com/forestscience/article-abstract/31/2/303/4656984

Černý, V., 1985. Thermodynamical approach to the traveling salesman problem: An efficient simulation algorithm. J. Optim. Theory Appl. 45, 41–51. https://doi.org/10.1007/BF00940812

Dong, L., Bettinger, P., Liu, Z., Qin, H., 2015. A comparison of a neighborhood search technique for forest spatial harvest scheduling problems: A case study of the simulated annealing algorithm. For. Ecol. Manag. 356, 124–135. https://doi.org/10.1016/j.foreco.2015.07.026

Dong, L., Lu, W., Liu, Z., 2020a. Determining the optimal rotations of larch plantations when multiple carbon pools and wood products are valued. For. Ecol. Manag. 474, 118356. https://doi.org/10.1016/j.foreco.2020.118356

Dong, L., Tian, D., Lu, W., Liu, Z., 2020b. Estimating the efficient parameter values of different neighborhood search techniques of simulated annealing in forest spatial planning problems. IEEE Access 8, 115905–115921. https://doi.org/10.1109/access.2020.3004563

Katakura, M., Yamanouchi, M., Furukawa, H., 2005. A study of long rotation management for artificial stands of Japanese cypress and Japanese larch (in Japanese). Bull. Nagano Prefect. For. Res. Cent. 19, 1–16. http://www.pref.nagano.lg.jp/ringyosogo/seika/kenkyu/ikurin/documents/iku-19-1.pdf

Kirkpatrick, S., Gelatt, C. D., Vecchi, M. P., 1983. Optimization by simulated annealing. Science 220, 671–680. https://doi.org/10.1126/science.220.4598.671

Koskela, E., Ollikainen, M., Pukkala, T., 2007. Biodiversity conservation in commercial boreal forestry: The optimal rotation age and retention tree volume. For. Sci. 53, 443–452. https://doi.org/10.1093/forestscience/53.3.443

Matsuoka, Y., Shirasawa, H., Hayashi, U., Aruga, K., 2021. Annual availability of forest biomass resources for woody biomass power generation plants from subcompartments and aggregated forests in Tohoku region of Japan. Forests, 12, 71. https://doi.org/10.3390/f12010071

Moriguchi, K., 2013. Comparison of solutions of three operations research methods for forest stand management. J. Jpn. For. Soc. 95, 199–205. https://doi.org/10.4005/jjfs.95.199

584 Moriguchi, K., 2020. Acceleration and enhancement of reliability of simulated annealing for
585 optimising thinning schedule of a forest stand. Comput. Electron. Agric. 177, 105691.
586 https://doi.org/10.1016/j.compag.2020.105691
587 Moriguchi, K., 2021. Identifying optimal forest stand selection under subsidisation using
588 stand-level optimal harvesting schedules. Land Use Policy 108, 105674.
589 https://doi.org/10.1016/j.landusepol.2021.105674
590 Moriguchi, K., Ueki, T., Saito, M., 2015. An evaluation of the use of simulated annealing to
591 optimize thinning rates for single even-aged stands. Int. J. For. Res. 2015, 1–15.
592 https://doi.org/10.1155/2015/173042
593 Moriguchi, K., Ueki, T., Saito, M., 2017. Identification of effective implementations of simulated
594 annealing for optimising thinning schedules for single forest stands. Eur. J. Oper. Res. 262,
595 1094–1108. https://doi.org/10.1016/j.ejor.2017.04.037
596 Moriguchi, K., Ueki, T., Saito, M., 2020. Establishing optimal forest harvesting regulation with
597 continuous approximation. Oper. Res. Perspect. 7, 100158.
598 https://doi.org/10.1016/j.orp.2020.100158
599 Nagano Prefectural Government., 2020. Standard unit cost table for silviculture project (fiscal
600 2020). https://www.pref.nagano.lg.jp/shinrin/sangyo/ringyo/seibi/zorin/index.html (Final
601 access: 30 Aug 2021)
602 Nghiem, N., 2014. Optimal rotation age for carbon sequestration and biodiversity conservation in
603 Vietnam. For. Polic. Econ. 38, 56–64. https://doi.org/10.1016/j.forpol.2013.04.001
604 Ota, T., Takahira, S., Nakama, K., Yoshida, S., Mizoue, N., 2013. Effectiveness of low-density
605 planting in terms of planting cost reduction and felling income reduction. J. Jpn. For. Soc. 95,
606 126–133. https://doi.org/10.4005/jjfs.95.126
607 Pasalodos-Tato, M., Pukkala, T., 2007. Optimising the management of even-aged *Pinus sylvestris* L.
608 stands in Galicia, north-western Spain. Ann. For. Sci. 64, 787–798.
609 https://doi.org/10.1051/forest:2007059
610 Roise, J. P., 1986. A nonlinear programming approach to stand optimization. For. Sci. 32, 735–748.

https://academic.oup.com/forestscience/article-abstract/32/3/735/4641929

Williams, J. S., Nautiyal, J. C., 1990. The long-run timber supply function. For. Sci. 36, 77–86. https://academic.oup.com/forestscience/article-abstract/36/1/77/4642570

Xue, H., Mäkelä, A., Valsta, L., Vanclay, J. K., Cao, T., 2019. Comparison of population-based algorithms for optimising thinnings and rotation using a process-based growth model. Scand. J. For. Res. 34, 458–468. https://doi.org/10.1080/02827581.2019.1581252

Yoshimoto, A., 2003. A dynamic programming model for forest stand management using MSPATH algorithm. Proc. Inst. Stat. Math. 51, 73–94. https://www.ism.ac.jp/editsec/toukei/pdf/51-1-073.pdf

Yoshimoto, A., Haight, R. G., Brodie, J. D., 1990. A comparison of the pattern search algorithm and the modified PATH algorithm for optimising an individual tree model. For. Sci. 36, 394–412. https://academic.oup.com/forestscience/article-abstract/36/2/394/4642620

Table 1. Calculation time for each yield model.

	Model	VA				EVA			
		A		B		A		B	
		Time (sec)	*n*	Time (sec)	*n*	Time (sec)	*n*	Time (sec)	*n*
SY	Cedar-F	0.88 ± 0.224	7	0.72 ± 0.227	7	2.64 ± 0.453	6	1.83 ± 0.255	6
	Cedar-H	0.31 ± 0.053	5	0.19 ± 0.039	5	0.22 ± 0.053	3	0.21 ± 0.040	3
	Cypress-F	0.70 ± 0.153	6	0.43 ± 0.075	6	1.08 ± 0.237	5	0.99 ± 0.167	5
	Cypress -H	0.10 ± 0.027	3	0.07 ± 0.016	3	2.04 ± 0.335	5	1.41 ± 0.240	5
	Larch-F	1.78 ± 0.290	8	1.44 ± 0.237	8	5.36 ± 1.079	7	3.46 ± 0.706	7
	Larch-H	0.15 ± 0.030	4	0.10 ± 0.025	4	0.29 ± 0.061	3	0.22 ± 0.053	3
	Pine-F	1.44 ± 0.346	7	1.20 ± 0.177	7	2.71 ± 0.539	6	1.70 ± 0.281	6
	Pine-H	0.74 ± 0.101	6	0.56 ± 0.079	6	0.56 ± 0.123	4	0.42 ± 0.065	4
	Mean	0.76		0.59		1.86		1.28	-
LY	Cedar-F	15.49 ± 3.935	7	16.08 ± 2.967	7	1.34 ± 0.340	4	1.34 ± 0.305	4
	Cedar-H	2.67 ± 0.817	5	5.29 ± 1.539	5	3.18 ± 0.730	5	4.22 ± 0.765	5
	Cypress-F	8.77 ± 5.930	6	4.04 ± 0.508	5	0.38 ± 0.130	3	0.44 ± 0.142	3
	Cypress -H	2.33 ± 0.692	5	4.24 ± 0.411	5	0.36 ± 0.067	3	0.38 ± 0.101	3
	Larch-F	34.46 ± 7.788	8	31.7 ± 7.641	8	1.23 ± 0.234	4	1.45 ± 0.335	4
	Larch-H	7.39 ± 1.593	6	11.29 ± 1.539	6	1.09 ± 0.219	4	1.49 ± 0.310	4
	Pine-F	17.17 ± 0.431	7	20.86 ± 1.408	7	13.10 ± 1.667	6	20.14 ± 3.295	6
	Pine-H	14.49 ± 2.877	7	16.72 ± 3.957	7	8.31 ± 2.523	6	14.03 ± 4.770	6
	Mean	12.85		13.78	-	3.62		5.43	-

Replicates: 10. *n*: The number of harvests at the end of the increment of *n*. Values shown are mean ± one standard deviation. Each optimization process used different random seeds.